

# Variability, predictability and prediction of DJF climate in NCEP Coupled Forecast System (CFS)

*P. Peng, Q. Zhang, A. Kumar, H. van den Dool, W. Wang, S. Saha and H. Pan*

[Peitao.Peng@noaa.gov](mailto:Peitao.Peng@noaa.gov)

(301) 763-8000 ext 7507 (voice)

(301) 763-8125(fax)

*CPC/NCEP/NOAA*

## 1. Introduction

Recently, the National Centers of Environment Prediction (NCEP) implemented a new coupled forecast system (CFS) for seasonal and interannual climate forecast. The CFS is a fully coupled model for global ocean, land and atmosphere. Its moderate climate drift in long-term integrations indicates a remarkable advancement in climate model development. Owing to its excellence in this respect, the CFS is able to forecast sea surface temperatures (SSTs) and climate simultaneously, having no need to adopt the widely used “two-tier” approach in which SSTs are predicted first and are then used to force the overlying atmosphere. In order to assess the skill of the CFS in climate forecast, a series of climate hindcasts have been conducted with the CFS for the period of 1981-2003. This hindcast dataset is not only useful for the forecast skill assessment, but also valuable for the study of some other issues in climate variability, predictability and predictions. With this dataset, we have investigated the following issues: (1) model climate drift in seasonal forecast and its dependence on the lead time of forecast; (2) variability and predictability of seasonal climate; (3) ENSO and its associated climate anomalies; (4) the

reality and the potential of the CFS skill in seasonal climate forecast. Our analysis starts from the DJF season and will be extended to other seasons. This paper presents the results of the DJF season only.

## 2. Hindcast and data

The hindcasts consist of *fifteen* 9-month integrations starting from the observed atmospheric and oceanic initial conditions for each month during the period of 1981-2003. For the target season DJF, the predictions from May through October, corresponding to six-month through one-month lead, are used for the analysis. The variables used in the analysis are SSTs, surface air temperature, precipitation rate and 200hPa height. The observational data used for the model verification include the OI (optimal interpolation) SST, CMAS surface air temperature, Xie-Akin precipitation and the reanalysis-2 200hPa height.

## 3. Results

(1) *Model climate drift and its dependence on the lead time of forecast*

The model climate drift refers to the deviation of the model climatology from the observational. The DJF climatology in this study is defined as the average of

the three-month mean over the winters of 1981/82 through 2003/04, being consistent with the period of the hindcasts. For the model, the DJF climatology is calculated separately for each lead time of forecast, so as to examine the dependence of the climate drift onto the lead. Fig.1 exhibits the climate drift for the one-month lead forecast, that is, for the forecast with October initial conditions. It is obvious that the drift of SST (upper panel) in the equatorial region is within  $1^{\circ}\text{C}$  only. As to be shown later, this moderate bias in basic state does not lead to serious errors in SST variability in that region. In some subtropical and mid-latitude regions, however, the bias is larger and even up to  $2^{\circ}\text{C}$ . Because the SST variation beyond the tropics is basically wind driven, the larger bias over there is likely due to the bias in surface wind. In contrast, the major bias of the model precipitation (middle panel) is in the tropics. It is characterized by the deficit in the Indonesia and northern Australia area and the equatorial Pacific and Atlantic Oceans. The surplus is seen along the north flank of all equatorial oceans and the south flank of equatorial Atlantic, Indian Ocean and eastern equatorial Pacific. The bias in mid-latitude storm-track regions is also evident but much weaker. As expected, for the boreal winter season major bias of the model 200hPa eddy height (lower panel) is in the middle and high latitudes of the northern hemisphere. The positive bias over the western and the northwestern Pacific and its downstream wavetrain-like patterns suggest the height bias is tropically forced by the precipitation (i.e., diabatic heating) bias over the tropical and subtropical western

Pacific. This conjecture has been proved by a linear stationary wave model forced with the tropical diabatic heating derived from the precipitation bias. The tropically forced wavetrain in the linear model resembles the height bias of the model very much (not shown). The connection between the bias in the tropical heating and that in the extratropical circulation implies that the correction of the former could lead to alleviation of the latter.

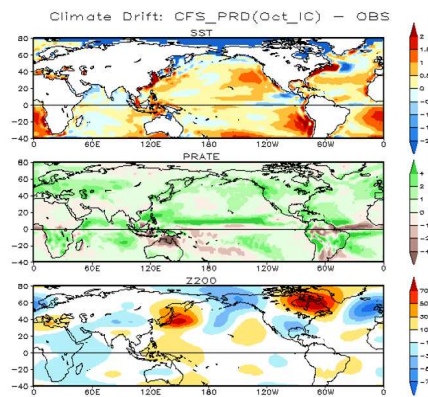


Fig.1 CFS climate drift in SST (upper), precipitation rate (middle) and 200hPa height (lower).

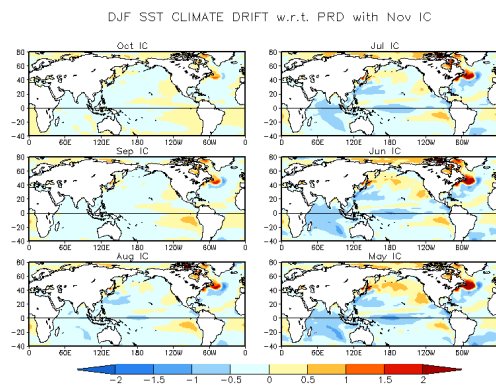


Fig.2. CFS climate drift in SST with respect to 0-month lead forecasts.

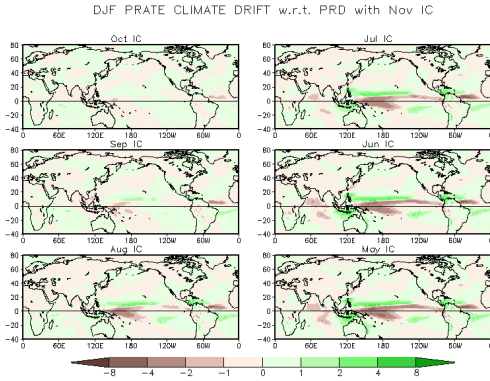


Fig.3. The same as Fig.2 but for precipitation rate.

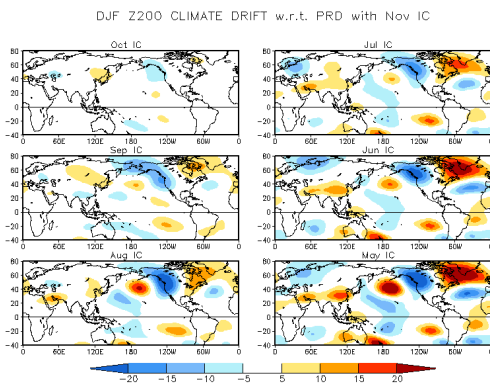


Fig.4. The same as Fig.2 but for eddy 200hPa height.

The dependence of the climate drift onto the lead time of forecast is shown in Fig.2 through Fig.4 for SST, precipitation and 200hPa eddy height, respectively. In order to present the lead time dependence more clearly, the deviations of the model climatology in these figures are with respect to the model climatology calculated with the 0-month lead forecasts (i.e., the forecasts with initial conditions in November), rather than with respect to the observational as in Fig.1. As lead time increases, the SST in the Indian Ocean and the equatorial Pacific gets colder and colder, with the magnitude to be around 1° C for the six-month lead in the central equatorial Pacific and the southeast Indian Ocean. The systematic cooling

can also be found in subtropical western Pacific and the midlatitude Atlantic. In the northeastern Pacific and some regions in the North Atlantic, however, the SST gets warmer and warmer. Comparing Fig.2 with Fig.1, it is interesting to see that the cooling tendency in the equatorial Pacific and the southeastern Indian Ocean tends to alleviate the SST bias in those regions, whereas the warming tendency tends to enhance the existing warm bias. The corresponding tendency in precipitation (Fig.3) is dominated by the dryness in the western and central equatorial Pacific and the wetness in the maritime islands and the north flank of the dryness, in response to the SST tendency in the tropics. The tendency in 200hPa eddy height (Fig.4) is obviously a wavetrain emanated from the tropics forced by the tendency in precipitation (i.e., diabatic heating). Comparing Fig.4 with Fig.2 we can speculate that the SST tendency in midlatitude oceans is driven by the circulation tendency through Ekman effect.

## (2) Variability and predictability of DJF climate

The analysis of climate variability begins with the variance (or standard deviation) of DJF mean with respect to climatology. In order to examine the dependence onto the lead time of forecast, the variance of the model forecasts is also calculated separately for each lead time, similar to the climatology calculation described earlier. The results are then compared with the observational. The variance of the model forecasts is further split into the part due to ensemble mean and the part due to the ensemble spread. The former

is regarded as “signal” and the latter as “noise” according to their predictability. The signal-to-noise ratio thus provides a quantitative measure of the predictability. The variability and predictability of 200hPa height are further assessed with the EOF analysis. The EOF modes explaining the total variance of the model forecasts (i.e., including both the ensemble mean and the spread) tell the ability of the model in generating the observed climate modes, and the results for the ensemble mean show the potentially predictable modes.

For SST, it is found that for one through six month lead, the variance of the model forecasts has caught most observed features, particularly in the tropics, but with slightly larger amplitude in the equatorial Pacific for one through four month lead (not shown). For the signal part, the variance decreases as lead time increases, while for the noise part it increases as lead time increases from one to three months and then becomes saturated. Fig. 5 presents the signal-to-noise ratio in terms of standard deviation. The ratio is characterized by the larger magnitude in the tropics and a maximum in the central and eastern equatorial Pacific, indicating that the tropical SST is more predictable than extratropical and the ENSO related variability is of the highest predictability. It is evident that as lead time gets longer, the signal-to-noise ratio becomes lower. This is basically due to the weakening of the signal. It is conceivable that the system will eventually lose predictability when lead time is long enough. The predictability estimation given here is more realistic than that given with the AMIP-type

ensemble run, because the latter is based on the assumption that boundary conditions are predictable. In other words, within the context of CFS we are studying the first kind of predictability--the initial condition problem, while with the AMIP-type run the second kind of predictability--the boundary forcing problem is examined.

For 200hPa height, the variance of the model forecasts well resembles the observed in pattern, but its intensity is moderately weaker in North Atlantic region and stronger in North Pacific region than the observed for all the leads (not shown). Similar to the SST case, the

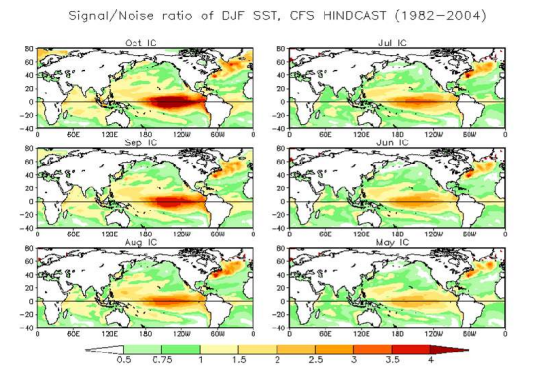


Fig.5. The signal-to-noise ratio of CFS SST forecasts.

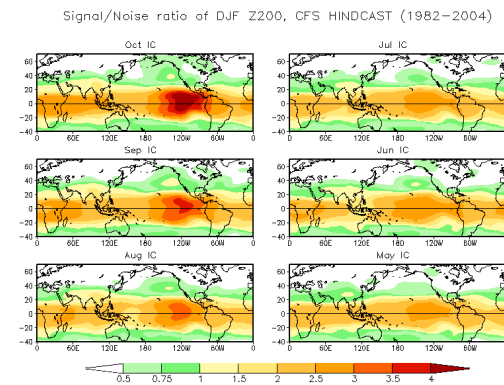


Fig.6. The signal-to-noise ratio of CFS 200hPa height forecasts.

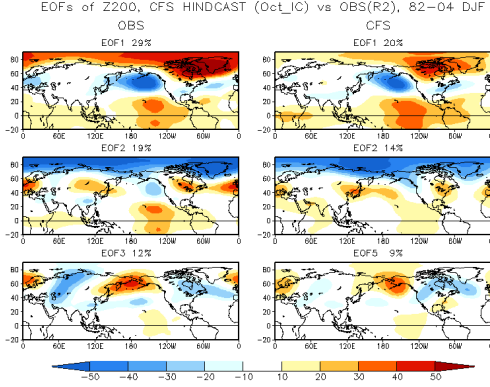


Fig.7. The first three EOF patterns of total variability of 200hPa height for observation (left) and CFS 1-month lead forecast (right).

200hPa height signal also decreases as the lead time increases, but the noise gets saturated at two-month lead, faster than the SST noise. Fig. 6 shows the signal-to-noise ratio. It is obvious that the high ratio occurs in low latitude and the PNA region, suggesting that ENSO related variability dominates the predictability of the atmosphere. As expected, the predictability decreases as lead time increases. By the lead of six months, the signal becomes comparable to the noise in the PNA region, indicating the gradual losing of predictability in that region. Fig.7 shows the first three EOF patterns of the observed and the one-month lead forecasted DJF 200hPa height. For the observations, (left panels), we can find the signatures of the TNH, PNA, NAO/AO, WPO and Eurasia modes in the three EOF patterns. The signatures of these modes can also be found in the EOF patterns of model forecasts (right panels). The resemblance of CFS to the observation in EOF patterns further demonstrated the ability of the CFS in generating the observed climate variability. The predictable modes are

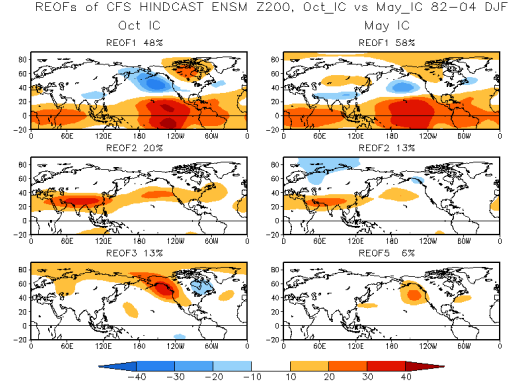


Fig.8. The first three EOF patterns of 200hPa height of CFS ensemble mean forecast. The left is for 1-month lead and the right is for 6-month lead.

shown in Fig.8, which presents the first three EOF patterns of the *ensemble mean* forecasts for 1-month lead (left panels) and 6-month lead (right panels). The spatial patterns of the EOFs in left panels are very similar to those in right panels, but the amplitude in right panels is weaker, consistent with the weaker signals in the 6-month lead forecast. The first EOF is obviously the ENSO teleconnection pattern, and the third EOF reflects the non-linearity of the teleconnections between El Niño and La Niña. The second mode is related to the warm trend in the India Ocean. Because the three EOFs have explained about eighty percent of the variance of the ensemble mean, the predictable DJF climate anomalies by CFS are basically tropically forced. In addition, the low degree of freedom revealed by the EOF analysis indicates the quasi-linear nature of the system.

### (3) ENSO and its associated climate anomalies

Since ENSO is the major source of the predictability of inter-annual climate variability, it is necessary to examine the

performance of CFS in forecasting ENSO related climate anomalies. Fig.9, Fig.10 and Fig.11 respectively show the composites of the observed and the model forecasted SST, precipitation rate and 200hPa height anomalies for ENSO winters. From these figures we can see that for 1-month lead, the model forecasts are very similar to the observational in both pattern and amplitude. For 6-month lead, however, westward shift and amplitude weakening happen to all the three fields. According to the ENSO teleconnection theory, the shift of the 200hPa height should be caused by the shift of the tropical precipitation, which in turn is caused by the shift of SST. The SST shift is likely related to the cold bias in the central equatorial Pacific shown in Fig. 2. The mechanism of the relation is not clear yet and is to be analyzed later. Comparing the left panels with the right panels in these three figures, we can see that climate anomalies in El Niño cases are almost anti-symmetric to those in La Niña cases. That means during this period the ENSO related climate variability are pretty linear.

In addition to the ensemble mean, we have also examined the variation of

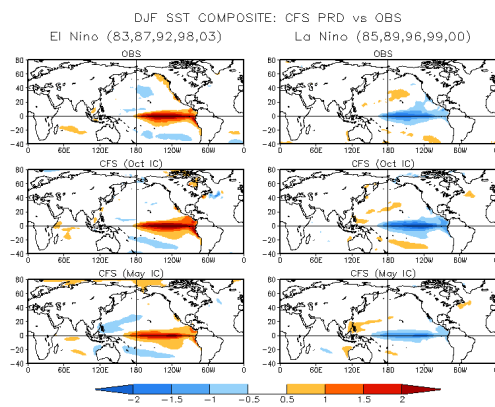


Fig.9. ENSO SST composite for observation (upper), 1-month lead forecast (middle) and 6-month lead forecast (lower). The left is for El Niño and the right for La Niña.

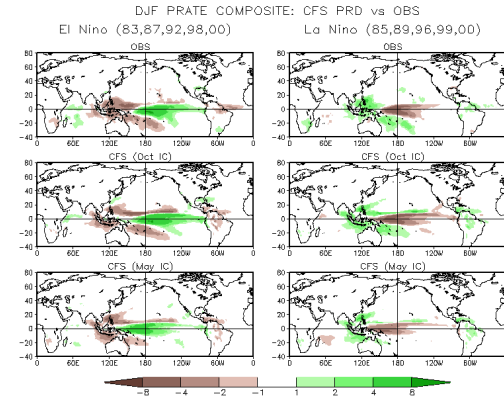


Fig.10. The same as Fig.9 but for precipitation rate.

Fig.11. The same as Fig.9 but for 200hPa height.

ensemble spread associated with ENSO. It is found that in North Pacific area the ensemble spread in La Niña winters is significantly bigger than that in El Niño winters (not shown). The result is consistent with that obtained from AMIP-type ensemble runs. Its implication in prediction is that in that area climate in El Niño winters is more predictable than in La Niña winters.

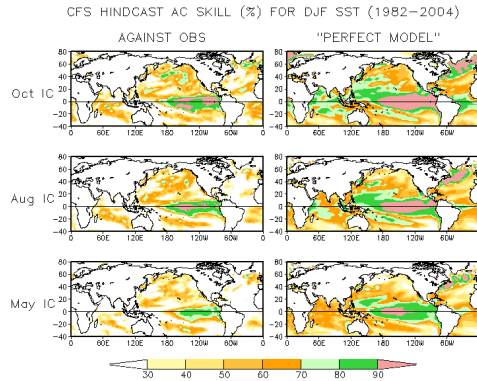


Fig.12. The CFS SST forecast skill verified against observation (left) and that based on the “perfect model assumption” (right) for lead time of 1-month (upper), 3-month (middle) and 6-month (lower).

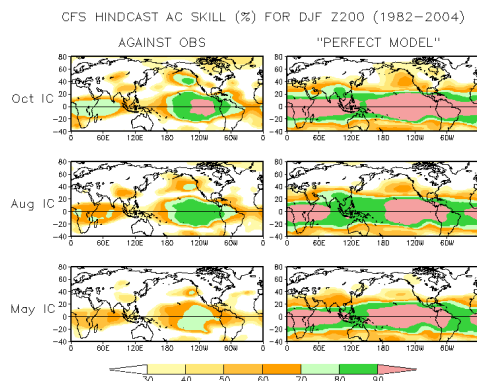


Fig.13. The same as Fig.12 but for 200hPa height.

*(4) Forecast skill: reality and potential*

The CFS forecast skill is simply measured with the temporal correlation between model forecast and observation. Considering the model is not perfect yet, there may be still a room for the skill improvement. In order to know the upper limit of the skill, we have calculated the potential skill based on the “perfect model assumption”, that is, take one ensemble member as “observation” and the other fourteen member ensemble as prediction. By repeating the calculation for all fifteen members and

taking the average of such obtained fifteen skill maps, we have a “perfect model” forecast skill. Though such a skill can be model dependent, owing to the high quality of CFS it may still provide a valuable estimation for the potential predictability of the seasonal climate. Figs.12 and 13 present the real and the potential skills for SST and 200hPa height, respectively. From these figures we can see the current CFS skills and its potential improvement.

**4. Summary**

- (a) Part of the CFS climate drift in the extratropics is likely forced by the drift in the tropics;
- (b) CFS climate drift increases moderately as lead time of forecast increases from one to six months;
- (c) ENSO dominates the predictable component of interannual climate variability;
- (d) In the period of 1982-2004, ENSO-related mean anomalies are pretty linear in both CFS and OBS. However, the spread of ensemble North Pacific region is bigger in La Nina winters than in El Nino winters;
- (e) CFS shows pretty high forecast skills for the tropics and appreciable skills for the extratropics with up to six-month lead time;
- (f) The decrease of forecast skills in the extratropics for longer lead is partially due to the westward shift of the ENSO teleconnection patterns in forecast, which in turn is caused by the westward shift of tropical SST and precipitation patterns;
- (g) The “perfect model” skills show us brighter future.

